

Effects of roughness on the stability of wall-bounded shear flows

Masahito Asai

Department of Aerospace Engineering, Tokyo Metropolitan University,
6-6 Asahigaoka, Hino, Tokyo 191-0065, JAPAN.

*E-mail of presenting author: masai@sd.tmu.ac.jp

Abstract Experiments on the effect of surface roughness of small height on the growth of Tollmien-Schlichting (T-S) waves are conducted. Two kinds of distributed roughness are considered. One is sinusoidal roughness and the other is rectangular roughness distributed in the streamwise direction. The results clearly demonstrate the destabilizing effect of two-dimensional distributed roughness in Blasius boundary layer and plane Poiseuille flow. It is also shown that when the roughness elements are distributed at an angle to the two-dimensional T-S waves, the destabilizing effect is markedly weakened compared with the two-dimensional distributed roughness.

Keywords Instability, Transition, Surface roughness, Tollmien-Schlichting waves

1. Introduction

It is known experimentally that surface roughness generally promotes laminar-turbulent transition in boundary layers. In past literatures^(1,2), the critical roughness height above which roughness can affect on the transition of Blasius boundary layer is often cited to be 25 in terms of the roughness Reynolds number $Re_k = U_k k / \nu$, where k is the roughness height, U_k is the Blasius flow velocity at the height k and ν is the kinematic viscosity. This criterion comes from extension of the hydraulic smooth concept in which the friction drag of turbulent flow departs from that for the smooth wall for $u^* k / \nu > 5$ where u^* is the friction velocity. However, the critical roughness condition for laminar-turbulent transition has not yet been clarified thus far, in particular, from stability and receptivity viewpoints.

If roughness is much larger than the critical height, each roughness element can lead to by-pass transition skipping the growth stage of Tollmien-Schlichting (T-S) waves through strong inflectional instability mechanism directly caused by roughness elements. When the roughness height is so small that the roughness little modifies the boundary layer profiles, on the other hand, its role in the transition process has not fully been understood except for isolated roughness. Isolated roughness of small height generally plays a role in the receptivity process⁽³⁾ where any departure from surface smoothness can excite T-S waves in cooperation with free-stream disturbances and acoustic

noise. For three-dimensional boundary layers, an isolated, three-dimensional roughness element itself works as an origin of stationary cross-flow instability mode developing into the so-called cross-flow vortices even when its height is extremely small.

In the case of distributed roughness, Corke et al⁽⁴⁾ compared amplification of T-S waves in zero-pressure gradient boundary layers on the smooth wall and on the rough wall under a natural disturbance condition experimentally. They used sand-paper roughness as the distributed roughness whose Reynolds number R_k was about 130. T-S waves grew more rapidly on the rough wall than on the smooth wall in their experiment. They found no appreciable difference in the velocity profile across the boundary layer between both the cases. Therefore they inferred that the faster growth of T-S waves on the rough wall was not attributed to a destabilizing effect of roughness such as an inflectional instability immediately behind an isolated roughness, and pointed out a possibility of continual excitation of T-S waves on the rough wall by freestream turbulence. However, it could not be clarified whether the faster growth of T-S waves observed was caused by increase of receptivity due to roughness or destabilization effect of roughness or both. The problem of the effects of distributed roughness on the stability and transition still remains open even now.

Recently our knowledge on the effect of distributed roughness has been improved in part. Floryan⁽⁵⁾ analyzed the stability of two-dimensional channel flow with two-dimensional distributed roughness of simple geometries by considering its spectral representation and showed that the two-dimensional distributed roughness of very small height whose Re_k was much less than 25 destabilized the flow to T-S waves. His theoretical prediction was verified experimentally by Asai and Floryan⁽⁶⁾. In their experiment, surface corrugation with amplitude of 4% of the channel half depth reduced the critical Reynolds number 5772 for the linear instability of plane Poiseuille flow down to about 4000.

In this paper, we explain our recent experiments on the effect of distributed surface roughness of small height on the T-S instability, in which two kinds of roughness geometry were considered. One is a wavy wall with small

amplitude (height) less than the critical roughness height ($Re_k < 12$). The other consists of rectangular roughness elements distributed in the streamwise direction. In the latter case, our particular focus was paid on the coupling between two-dimensional T-S waves and oblique roughness elements to clarify how critically the destabilizing effect may depend on the oblique angle of roughness elements.

2. Surface corrugation

The experiment was conducted in a low turbulence wind tunnel of open jet type, with a test section of $400 \times 400 \text{ mm}^2$ in cross section. Two Plexiglas sidewalls maintain the two-dimensionality of the main stream and the upper area is covered with 24-mesh gauze instead of rigid wall to realize the boundary layer with zero pressure gradient without developing a mixing layer from the tunnel exit. A boundary-layer plate of 1195mm long was set parallel to the oncoming uniform flow in the test section. As illustrated in Fig. 1, the boundary-layer plate consists of a brass plate of 5mm thick and 300mm long with a sharp leading edge, followed by a Plexiglas plate of 20mm thick and 895mm long. The Plexiglas plate can be replaced with a plate with surface corrugation or a smooth surface plate. As for the coordinate system, x is the streamwise distance measured from the leading edge, y the normal-to-wall distance and z the spanwise distance.

The surface corrugation whose shape is given as $y_w = A \sin(\alpha_w x)$ where the wavelength $2\pi/\alpha_w$ is 32mm and the amplitude A is 0.21mm. The corrugation wavelength is the order of T-S wavelengths in the present experiment. The surface corrugation (wavy wall) ranges from $x=320\text{mm}$ to $x=1024\text{mm}$, a distance of 22 wavelengths.

T-S waves of a single frequency were excited by means of vibrating ribbon technique. The vibrating ribbon was stretched in the spanwise direction at a height of 1mm at a streamwise location 190mm downstream from the leading edge. Twelve pieces of Neodymium magnets were installed on the opposite side of the boundary layer plate to generate a magnetic field perpendicular to the ribbon. The input current to the ribbon was supplied with a signal generator through a power amplifier. A constant-temperature hot-wire anemometer was used to measure time-mean and fluctuating streamwise velocity components, denoted by U and u , respectively.

Detailed experiments were conducted at the free-stream velocity $U_\infty = 3\text{m/s}$ and 6m/s . Free-stream turbulence was less than 0.1% of U_∞ at the inlet of the test section. The streamwise variation of freestream velocity was less than 0.5%, which guaranteed the laminar boundary layer under zero pressure gradient. The Reynolds numbers based on the displacement thickness $R^* (=U_\infty \delta^* / \nu)$ were 320 and 460 at $x=190\text{mm}$ (the vibrating ribbon location) for $U_\infty = 3\text{m/s}$ and 6m/s , respectively. The ratio of the corrugation amplitude to the displacement thickness A/δ^* changed from 9.3% to 5.5% and from 13.2% to 7.8% over the distance $x=320\sim 920\text{mm}$ at $U_\infty = 3\text{m/s}$ and at $U_\infty = 6\text{m/s}$, respectively.

Fig. 2 displays the y -distributions of streamwise velocity U at $x=346\text{mm}$, 600mm and 856mm in the boundary layer on the smooth wall at $U_\infty = 6\text{m/s}$ by comparing with the Blasius flow profile. The velocity distributions coincide with the Blasius profile almost completely. Note that the sharp leading edge allows the Blasius flow to develop immediately downstream from the leading edge.

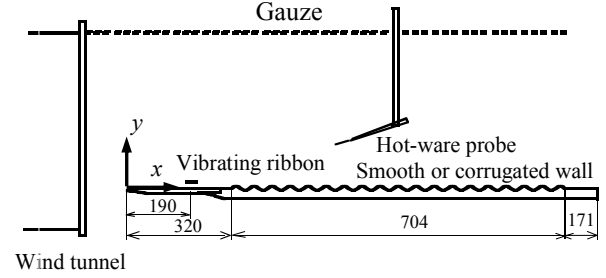


Fig. 1. Schematic diagram of test section.

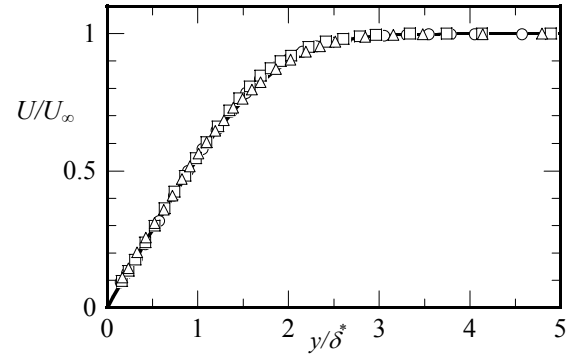


Fig. 2. The y -distributions of U in flat-plate boundary layer at $U_\infty=6\text{m/s}$. \circ $x=344\text{mm}$ ($xU_\infty/\nu=1.31 \times 10^5$), \square $x=600\text{mm}$ ($xU_\infty/\nu=2.28 \times 10^5$), \triangle $x=856\text{mm}$ ($xU_\infty/\nu=3.25 \times 10^5$). — Blasius flow

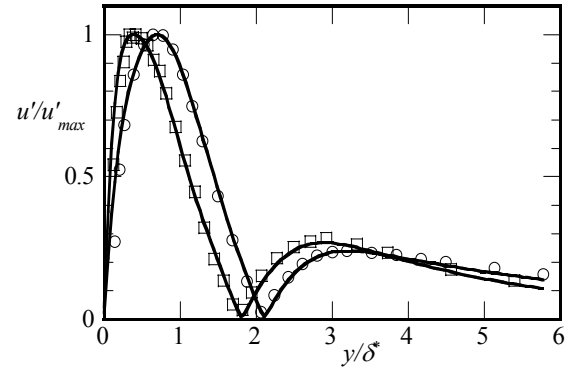


Fig. 3. Amplitude distributions of T-S wave excited at $F=1.5 \times 10^{-4}$ in flat-plate boundary layer at $U_\infty=6\text{m/s}$. \circ $x=310\text{mm}$ ($xU_\infty/\nu=1.18 \times 10^5$), \square $x=728\text{mm}$ ($xU_\infty/\nu=2.76 \times 10^5$). — Eigenmode of Orr-Sommerfeld equation.

When the vibrating ribbon was driven at a single frequency f , a two-dimensional T-S wave was excited, as verified in Fig. 3 which compares the y -distributions of r.m.s. value of the streamwise velocity fluctuation u (the forcing frequency component were singled out) with the

distribution of T-S wave calculated from the Orr-Sommerfeld equation.

Figs. 4(a) and (b) compare the streamwise development of T-S waves excited with non-dimensional frequency $F (=2\pi f\nu/U_\infty^2) = 1.5 \times 10^{-4}$ and 1.9×10^{-4} respectively between the cases of smooth wall and corrugated wall at $U_\infty = 6\text{m/s}$ in terms of the streamwise variation of the maximum r.m.s amplitude u'_m . The comparisons show that the surface corrugation surely enhanced the amplification of T-S wave even when the corrugation amplitude is only of the order of $0.1\delta^*$. We examined the disturbance development for various frequencies at $U_\infty = 3\text{m/s}$ and 6m/s and plotted the neutral stability locations where the disturbance ceased to grow (or decay) on the neutral stability diagram of Blasius flow obtained by the parallel flow theory (the Orr-Sommerfeld equation) and the non-parallel stability theory⁽⁷⁾ in Fig. 5. The surface corrugation causes the lower branch of the neutral curve moves towards smaller R^* and the upper branch towards higher R^* . Furthermore, we notice that the influence of surface corrugation is more pronounced for higher frequency T-S waves than lower frequency waves. This is attributed to the fact that for higher frequencies, the T-S wave passes across the lower and upper branches earlier and thus the corrugation amplitude relative to the displacement thickness A/δ^* is larger at the neutral locations than that for the case of lower frequencies. It is also important to point out that the development of T-S wave is decisively dominated by the behavior of the viscous Stokes layer very close to the wall. The Stokes-layer thickness is of the order of $(\nu/\omega)^{1/2}$ where $\omega = 2\pi f$ and thus T-S waves with higher frequency can be affected by the surface corrugation more strongly.

3. 2D and oblique roughness elements

This experiment was conducted in plane channel flow by using a rectangular wind channel of aspect ratio 26.7 whose width, height and length were 400mm, 15mm ($= 2h$) and 6300mm, respectively. The channel facility is the same as that used in the stability experiment by Asai and Floryan⁽⁶⁾ except extension of the streamwise length by 300mm. The laminar flow could be maintained up to the Reynolds number $R = 6500$. Here the Reynolds number is defined on the center-line velocity U_c and the channel half-height h ($= 7.5\text{mm}$).

The schematic diagram of the test section is illustrated in Fig. 6. The experiment was conducted at $R=5000$, which is subcritical for the linear instability in plane Poiseuille flow between two parallel smooth walls. The background turbulence was about 0.1% of U_c . Two-dimensional wave disturbances were excited through two transverse slots 300mm long and 3mm wide in the lower wall, located about $700h$ downstream from the channel inlet. The slots were covered with a thin aluminum plate in which many small holes of 0.4mm diameter were drilled spaced 0.6mm apart in the streamwise and spanwise directions. Each slot was connected with a loudspeaker through a specially

designed converging vane. Two loudspeakers were driven at a single frequency by using sine-wave generator through

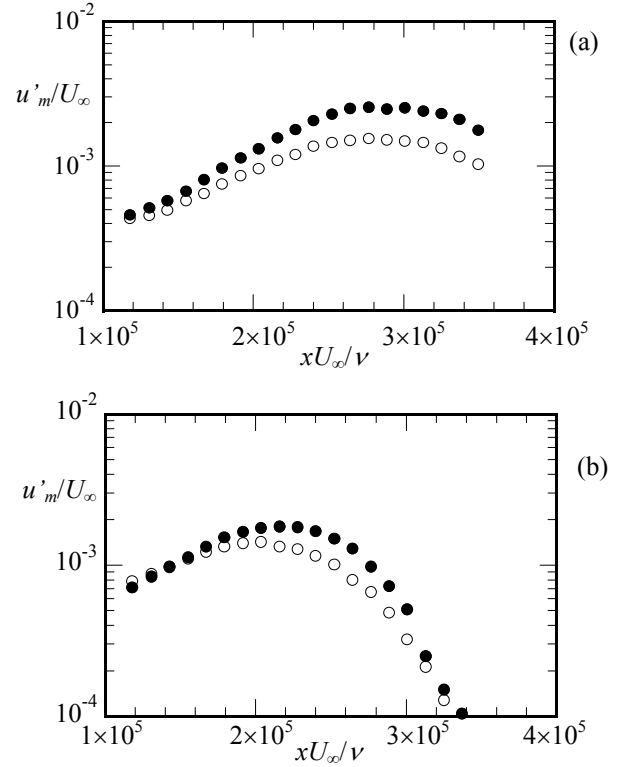


Fig. 4. Streamwise development of T-S waves at $U_\infty = 6\text{m/s}$. (a) $F = 1.5 \times 10^{-4}$, (b) $F = 1.9 \times 10^{-4}$. \circ ; Smooth wall. \bullet ; Corrugated wall.

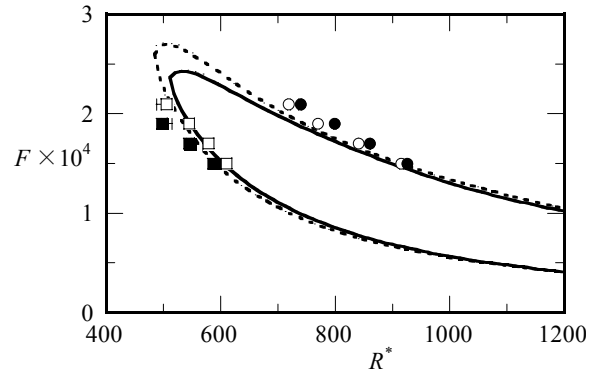


Fig. 5. Comparison of neutral stability locations for smooth wall (\square , \circ) and corrugated wall (\blacksquare , \bullet) at $U_\infty = 6\text{m/s}$ (\circ , \bullet) and $U_\infty = 3\text{m/s}$ (\square , \blacksquare). Solid curve; parallel flow theory. Broken curve; non-parallel theory⁽⁷⁾.

a power amplifier. The input signals to the two loudspeakers had an equal intensity but were 180° out of phase so that the suction and blowing occurring simultaneously at each instant of time did not affect the mass flow rate through the channel at all and therefore

cancelled acoustic monopole disturbances. In the (x, y, z) coordinate system, x is the streamwise distance measured from the location of downstream slot, y the normal-to-the-wall distance and z the spanwise distance. Fig. 7 compares the amplitude distribution of u excited by the disturbance generator mentioned above with the T-S wave calculated by the linear stability theory, showing that the T-S wave could be successfully introduced into the flow. Rectangular roughness elements were glued in equal interval on the lower wall ($y/h = -1$), some distance downstream from the disturbance generator. The height of each roughness element is 0.3mm, i.e., $0.04h$, and the width is 4.7mm ($= 0.67h$). Here it is noted that the channel walls were not completely smooth but possessed inevitable small deformation or irregularity. The magnitude of such surface irregularity was at most 0.02mm, which is one order of magnitude less than that of the present roughness elements. Two kinds of roughness arrangement were adopted here. One is two-dimensional arrangement, where roughness elements were glued at the right angle to the basic flow, as illustrated in Fig. 8(a). The other is of oblique roughness, as illustrated in Fig. 8(b). As for the two-dimensional roughness, the streamwise spacing of roughness elements L was 9.4mm, twice the roughness width. Therefore the nondimensional streamwise wavenumber $\alpha_w = 2\pi h/L$ is 5.0. For the experiment on the oblique roughness, each roughness element was glued with an oblique angle of 30° to the z -axis. The spacing in the direction normal to each roughness element was 9.4mm, the same as that in the two-dimensional case. The roughness region started at $x/h = 28$ and 14 for the cases of 2D roughness and oblique roughness, respectively.

Floryan⁷⁾ showed theoretically that two-dimensional rectangular roughness could also destabilize the flow for T-S waves similar to the case of sinusoidal roughness geometry. In the present experiment, our particular attention is focused on the dependency of the streamwise growth of T-S waves on the oblique angle of roughness elements. Fig. 9 compares the streamwise development of T-S waves excited at a non-dimensional frequency ω ($= 2\pi h/U_c$) = 0.33 for the flows with and without roughness elements. The two-dimensional roughness elements surely destabilize the flow even for the roughness height is only 4% of the channel half height which corresponds to the roughness Reynolds number R_k of 16. When the roughness elements were slightly oblique to the traveling (T-S) wave, the destabilizing effect of roughness elements is weakened compared with the two-dimensional arrangement of roughness elements.

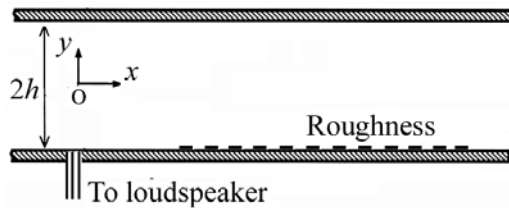


Fig. 6. Schematic diagram of test section.

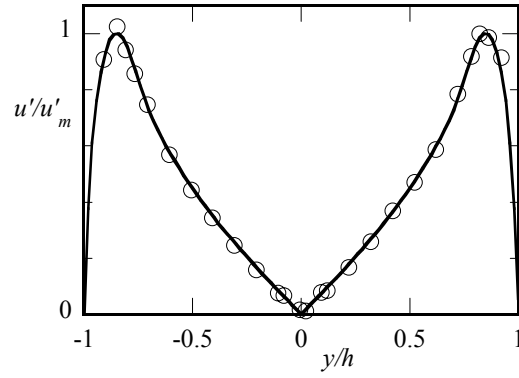


Fig. 7. Amplitude distribution of T-S wave excited at $\omega h/U_c = 0.27$ at $x/h = 100$ in the smooth wall channel at $R = 5000$. \circ Experiment, — linear stability theory.

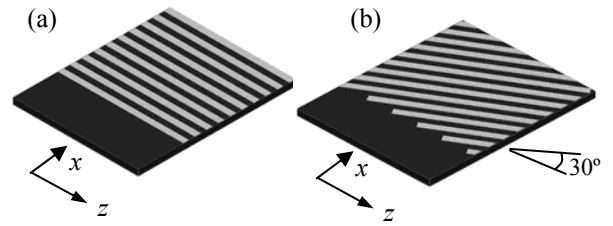


Fig. 8. Illustrations of 2D and oblique roughness arrangements.

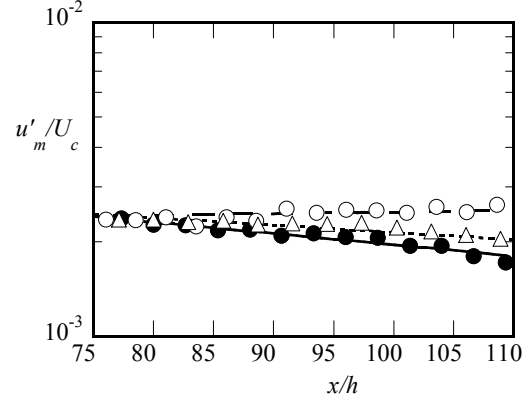


Fig. 9. Development of T-S waves ($\omega h/U_c = 0.33$) with and without roughness at $R = 5000$. \bullet ; Smooth wall. \circ ; 2D roughness. Δ ; oblique roughness.

Fig. 10 shows such a dependency of the instability on the arrangement of roughness elements by comparing with the growth rates of T-S waves against the non-dimensional frequency ($\omega h/U_c$) for the three cases, i.e., smooth wall, two-dimensional roughness and oblique roughness. The growth rates for the case of oblique roughness arrangement are not so different from those for the smooth wall case. Thus, the effect of distributed roughness is rather sensitive to the arrangement of roughness elements.

4. Concluding remarks

In this paper, our recent experimental results on the effect of distributed roughness on the Tollmien-Schlichting instability, conducted in Blasius boundary layer and plane Poiseuille flow, were presented. The experiment clearly showed the destabilizing effect of two-dimensional surface corrugation and distributed rectangular roughness. It was also found that when the roughness elements were distributed at a small angle to the two-dimensional T-S waves, the destabilizing effect was markedly weakened compared with two-dimensional roughness distribution. Indeed, when the roughness elements were arranged at an oblique angle of 30° , the growth rates of T-S waves tended to those in plane Poiseuille flow without roughness. Thus, the effect of distributed roughness highly depends on the arrangement of roughness elements.

Acknowledgments

The author would like to thank my coworkers, Dr. A. Inasawa, Mr. M. Shigeta and Mr. H. Suzuki who have contributed to the experimental studies presented in this paper. The author also thanks Prof. J.M. Floryan, Univ. Western Ontario for his theoretical support.

This work was in part supported by the Grant-in-Aid for Scientific Research from the Japan Society for Promotion of Science (No. 21560820), the Grant for Core Research for Evolutional Science and Technology from Japan Science and Technology Agency and the Grant for Scientific Research from Tokyo Metropolitan Government.

References

- [1] Morkovin, M.V.: On roughness-induced transition: facts, views and speculations. In *Instability and Transition* (eds. M.Y.Hussaini and R.G.Voigt), vol. 1, Springer-Verlag, 1990, 281-29.
- [2] Reshotko E.: Disturbances in a laminar boundary layer due to distributed surface roughness. In *Turbulence and Chaotic Phenomena* (ed.T.Tatsumi), Elsevier, 1984,. 39-46.
- [3] Saric W.S., Reed H.L. and Kerschen E.J.: Boundary-layer receptivity to free-stream disturbances. *Ann. Rev. Fluid Mech.*, 34 (2002) 251-276.
- [4] Corke T.C., Sever A.Bar and Morkovin M.V.: Experiments on transition enhancements by distributed roughness. *Phys. Fluids* 29 (1986) 3199-3213.
- [5] Floryan J.M.: Two-dimensional instability of flow in a rough channel. *Phys. Fluids*, 17 (2005) 044101/8.
- [6] Asai M. and Floryan J.M.: Experiments on the linear instability of flow in a wavy channel. *Eur. J. Mech./B Fluids*, 25 (2006) 971-986.
- [7] Gaster M.: On the effects of boundary-layer growth on flow stability. *J. Fluid Mech.*, 66 (1974) 465-480.

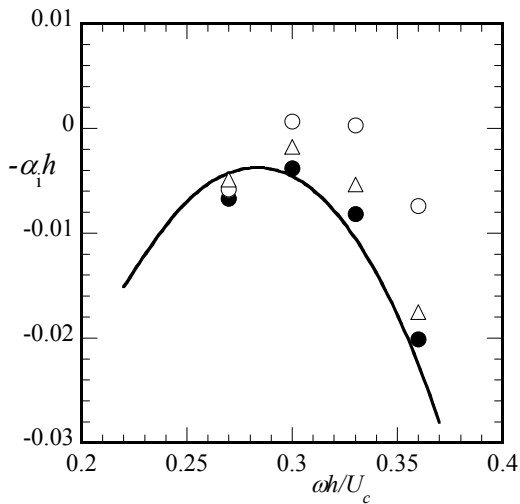


Fig. 10. Comparison of growth rates with and without roughness at $R=5000$. Solid curve; linear stability theory for plane Poiseuille flow. ●; Smooth wall. ○; 2D roughness. △; oblique roughness. Solid curve; the growth rates of plane Poiseuille flow.